Journal of Biomolecular NMR, 4 (1994) 775–785
ESCOM

J-Bio NMR 211

A spectral correlation function for efficient sequential NMR assignments of uniformly ^{15}N-labeled proteins

Christian Bartels and Kurt Wüthrich

Institut für Molekularbiologie und Biophysik, Eidgenössische Technische Hochschule-Hönggerberg, CH-8093 Zürich, Switzerland

Received 10 May 1994
Accepted 5 July 1994

Keywords: Proteins; Sequential resonance assignment; Interactive software XEASY

SUMMARY

A new computer-based approach is described for efficient sequence-specific assignment of uniformly ^{15}N-labeled proteins. For this purpose three-dimensional ^{15}N-correlated [^{1}H,^{1}H]-NOESY spectra are divided up into two-dimensional ^{1}H-^{1}H strips which extend over the entire spectral width along one dimension and have a width of ca. 100 Hz, centered about the amide proton chemical shifts along the other dimension. A spectral correlation function enables sorting of these strips according to proximity of the corresponding residues in the amino acid sequence. Thereby, starting from a given strip in the spectrum, the probability of its corresponding to the C-terminal neighboring residue is calculated for all other strips from the similarity of their peak patterns with a pattern predicted for the sequentially adjoining residue, as manifested in the scalar product of the vectors representing the predicted and measured peak patterns. Tests with five different proteins containing both α-helices and β-sheets, and ranging in size from 58 to 165 amino acid residues show that the discrimination achieved between the sequentially neighboring residue and all other residues compares well with that obtained with an unguided interactive search of pairs of sequentially neighboring strips, with important savings in the time needed for complete analysis of 3D ^{15}N-correlated [^{1}H,^{1}H]-NOESY spectra. The integration of this routine into the program package XEASY ensures that remaining ambiguities can be resolved by visual inspection of the strips, combined with reference to the amino acid sequence and information on spin-system types obtained from additional NMR spectra.

INTRODUCTION

Obtaining complete sequence-specific ^{1}H NMR assignments for a polypeptide chain opens the avenue to three-dimensional protein structure determination in solution (Wüthrich et al., 1982; Wüthrich, 1986). Today, two conceptually different assignment approaches for the identification of the resonances of pairs of sequentially neighboring amino acid residues use either homonuclear

Abbreviations: 1D, 2D, 3D, 4D, one-, two-, three-, four-dimensional; NOE, nuclear Overhauser enhancement; NOESY, nuclear Overhauser enhancement spectroscopy; COSY, correlation spectroscopy; TOCSY, total correlation spectroscopy.

^{1}H-^{1}H NOEs in natural unlabeled or recombinant isotope-labeled proteins, or heteronuclear scalar couplings in uniformly ^{13}C,^{15}N-doubly labeled proteins (e.g., Wüthrich, 1989; Bax and Grzesiek, 1993). Although the sequential NOE technique (Billeter et al., 1982; Wagner and Wüthrich, 1982) routinely relies entirely on homonuclear ^{1}H NMR for studies of small proteins, and has in a few cases also been used in this way for complete assignments of proteins from natural sources that contain more than 100 residues (e.g., Rico et al., 1989; Gao and Burkhart, 1991), its general use for larger proteins has to rely on isotope labeling and heteronuclear-resolved 3D and possibly 4D experiments. In contrast to the technique using heteronuclear scalar couplings, the NOE approach can be used for proteins uniformly labeled only with ^{15}N, which is of interest in many projects. The result of the analysis of the 3D ^{15}N-correlated [^{1}H,^{1}H]-NOESY spectra is then usually presented in the form of a 2D, sequentially ordered array of ^{1}H-^{1}H strips, each of which is centered about the amide proton shift along one frequency axis, and which are taken from the different spectral planes separated along the ^{15}N chemical shift axis (Fig. 1) (Driscoll et al., 1990; Wüthrich et al., 1991). To arrive at this final result, however, one has to go through a large number of pairwise comparisons of strips. For example, under the experimental conditions chosen for our studies of the 165-residue protein cyclophilin (Wüthrich et al., 1991; Spitzfaden et al., 1994) there were 12 246 pairs of strips to be analyzed. This paper describes a computer-based approach which enables automated identification of the strips corresponding to the sequential neighbors for over 50% of all residues in proteins with up to at least 160 residues. For nearly all of the remaining residues, our approach identifies a small number of strips (in most instances two to four) as representing likely sequential neighbors.

SPECTRAL CORRELATION FUNCTION FOR IDENTIFICATION OF SEQUENTIAL CONNECTIVITIES

Although similar approaches may be used for other types of 3D and 4D NMR spectra (see Introduction), we focus here on the analysis of 3D ^{15}N-correlated [^{1}H,^{1}H]-NOESY spectra. Using the program XEASY*, strips of the type shown in Fig. 1 are picked at the ^{15}N-H^N correlation peak of each residue. These strips extend over the entire spectral width along one ^{1}H chemical shift axis (ω_2 (^{1}H) in Fig. 1). The problem to be solved is for a given strip of residue s to identify one, or possibly several, strips k that are likely to represent the sequentially neighboring residue s+1. Thereby, strips of sequentially following residues are primarily recognized by the appearance of sequential $d_{\alpha N}$ and d_{NN} NOE cross peaks in the strip k, and by the fact that due to the spatial proximity of H^N_s and H^N_{s+1}, the strips of neighboring residues contain generally similar peak patterns. However, as is described below, a reliable correlation function for the identification of neighboring strips cannot be based directly on the measured peak intensities but requires some intricate empirical weighting of the relative intensities of different classes of peaks in the strips.

*XEASY is a new interactive graphics program for use on computers with the X-window system. In addition to the capabilities of the earlier software EASY (Eccles et al., 1991), it is devised for efficient handling of three- and higher-dimensional NMR spectra, and the presently described correlation function approach is implemented in XEASY. The program can be obtained by writing to the authors.

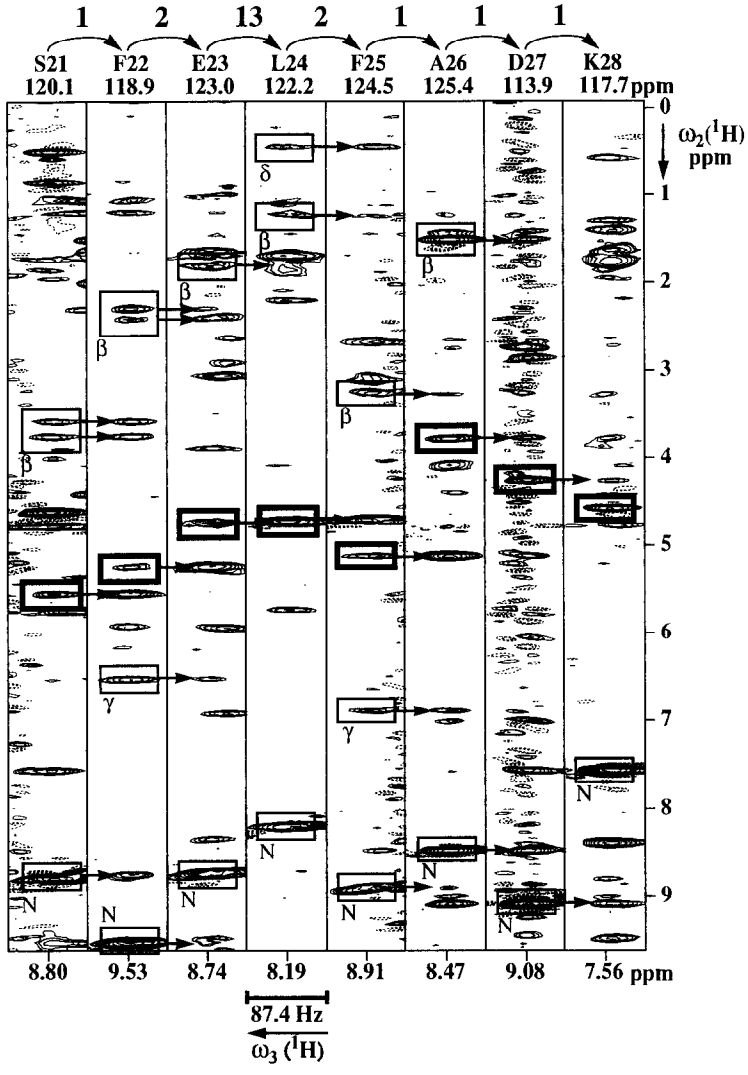

Fig. 1. Strips of the sequentially neighboring residues 21–28 of human cyclophilin in the complex with cyclosporin A, taken from the 600 MHz 3D ^{15}N-correlated [^{1}H,^{1}H]-NOESY spectrum (Wüthrich et al., 1991; Spitzfaden et al., 1994). Each strip is positioned at the amide ^{15}N frequency in ω_1 (listed above each strip) and centered about the amide proton frequency in ω_3 (listed below each strip) of the residue indicated at the top by the one-letter amino acid code and the sequence number. The width of the strips and the direction of ω_3 are indicated at the bottom of the figure. Positive and negative intensities are indicated with solid and dashed contours, respectively. The bold boxes in the strips contain the intraresidual H^N-H^α peaks, which are explicitly modified for the calculation of the spectral correlation function (see text and Fig. 2). Additional boxes identify the ^{15}N-H^N peaks (N) and intraresidual peaks with side-chain protons in residue s (assigned with Greek letters) for which corresponding sequential NOE connectivities to residue s+1 are observed (arrows). The result of the correlation function approach is indicated at the top, where the numbers above the curved arrows represent the ranks predicted by Eq. 1 for each residue s+1, relative to the preceding residue s (see text).

For the formulation of the spectral correlation function C(s+1,k), the peak patterns in each strip are represented as n-dimensional vectors $\vec{v} = (i_1,i_2,..,i_n)$, where i represents intensities derived

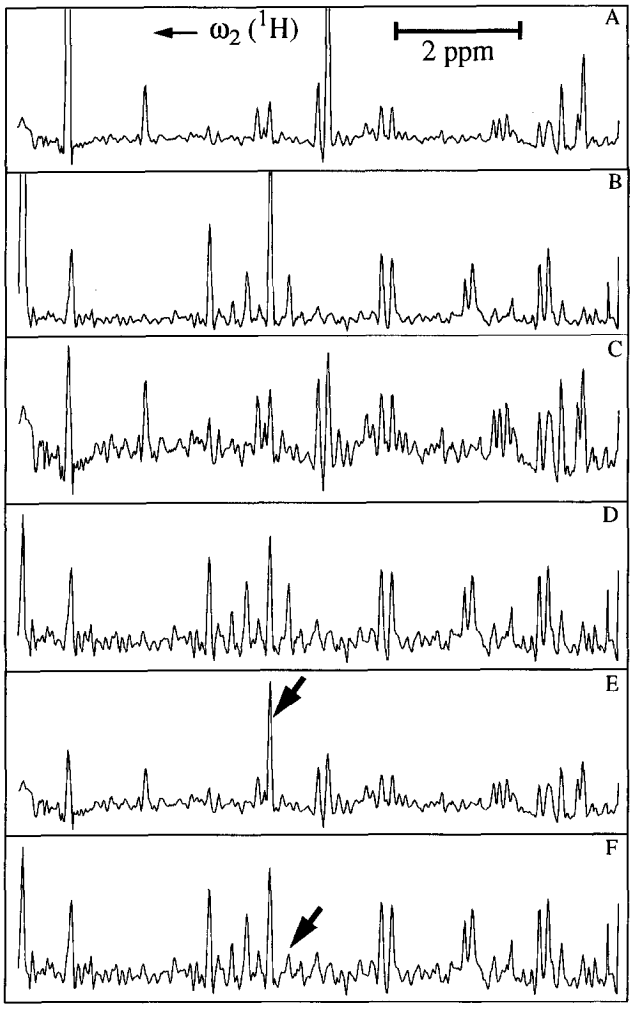

Fig. 2. (A) and (B): Cross sections along ω_2 (^{1}H), taken at the H^N frequencies along ω_3 (^{1}H) from the strips of Ser^{21} and Phe^{22} in Fig. 1. (C) and (D): Peak patterns derived from the experimental cross sections (A) and (B), respectively, by scaling all peak intensities according to Eq. 2. (E) Predicted peak pattern for the sequential neighbor of Ser^{21}, $\vec{v}_{s+1}$, derived from (A) according to Eq. 3. (F) Peak pattern for $\vec{v}_k = \vec{v}$ (Phe^{22}), derived from (B) according to Eq. 3. The arrows in (E) and (F) point to the peaks that were selectively scaled by the factor A in Eq. 3. The traces (E) and (F) were used in Eq. 1 to evaluate the rank of $\vec{v}$ (Phe^{22}) = $\vec{v}_k$, relative to $\vec{v}_s = \vec{v}$ (Ser^{21}) (see text).

from those measured in the ^{15}N-correlated [^{1}H,^{1}H]-NOESY spectrum, and n is the number of data points along ω_2 (^{1}H) (see Fig. 1). We then define

$$C(s+1,k) = \frac{\vec{v}_{s+1} \cdot \vec{v}_k}{|\vec{v}_{s+1}| \cdot |\vec{v}_k|} \tag{1}$$

Here, $\vec{v}_{s+1}$ represents the peak pattern predicted for the residue following residue s in the sequence, which is compared to strips $\vec{v}_k$ that are actual candidates for representing the residue s+1. The strip $\vec{v}_k$ with the highest value of C(s+1,k) is then identified as the first rank candidate

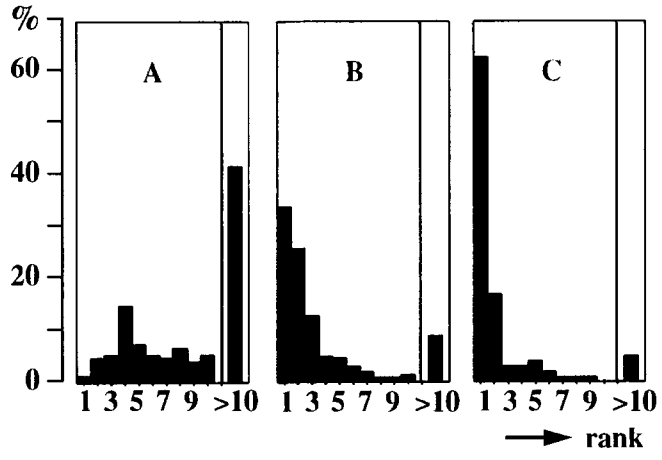

Fig. 3. Influence of the peak pattern scaling by Eqs. 2 and 3 (Fig. 2) on the performance of the spectral correlation function with cyclophilin. The histograms show the percentages of actual sequential neighbors that were attributed ranks 1–10 and >10 with the use of Eq. 1. (A) Experimental intensities of Fig. 2A and B were used to calculate the correlation function C(s+1,k) (Eq. 1). (B) Intensities scaled with Eq. 2 (Fig. 2C and D). (C) Intensities scaled with Eq. 3 (Fig. 2E and F).

for the sequential connectivity, and subsequent strips are ranked according to decreasing values of C(s+1,k). In the implementation in the program XEASY, the user selects a strip s and all the other strips in the 3D spectrum are then sorted according to the values of C(s+1,k).

Using the known sequential neighbors Ser^{21} and Phe^{22} in cyclophilin (Fig. 1) as an illustration, Fig. 2 shows how we obtain the peak patterns $\vec{v}_{s+1}$ and $\vec{v}_k$, to be used in Eq. 1. The procedure starts with the assumption, based on the close spatial proximity of H^N_{s+1} to the residue s, that the peak pattern of residue s (Ser^{21} in Fig. 1) can be used in an initial approximation to represent the predicted pattern $\vec{v}_{s+1}$. When the peak pattern $\vec{v}_{s+1} = \vec{v}_s$ (Ser^{21}) and all the patterns $\vec{v}_k$ are used with the experimental peak intensities (cross sections A and B in Fig. 2), the resulting value of C(s+1,k) is 0.018, which confers rank 14 to Phe^{22}. On average for all residues in cyclophilin, the rank of the strip corresponding to the sequentially following residue found with this approximation was 14.8 (Fig. 3A), which is clearly unsatisfactory. Therefore, the correlation function was further refined in the following two steps:

(1) Compared to earlier analyses of sequential NOEs (Billeter et al., 1982), the function in Eq. 1 gives too much weight to intense peaks. To suppress this systematic error, the individual peaks in the strips are scaled so that all peaks have similar absolute intensities but retain the original peak shapes. To this end, the computer identifies the data points p_m which correspond to maxima of the absolute intensity, and for each of these maxima the nearest local minima of the absolute intensity at low and high field, p_l and p_h (an intensity maximum is identified at each data point for which both neighboring data points have lower intensity, and a corresponding criterion is used to identify the intensity minima). For each intensity maximum we then have the scaling function

$$i_j = \frac{i_j^{ex}}{|i_m| + i_b} \qquad (p_l \leq j < p_h) \tag{2}$$

where i_j^{ex} is the experimental intensity (Fig. 2A and B), i_m the experimental intensity at p_m, i_b

a constant term that accounts for the noise level in the experimental spectrum (for all the spectra used here, the standard deviation of the noise was between 90 and 140, and $i_b = 1500$ was used in all the applications presented in this paper), and j runs over all data points between the two intensity minima. With this modification an impressive improvement was obtained for the ranking of sequentially neighboring strips in cyclophilin (Fig. 3B): about 30% of the sequential neighbors were identified as such (rank 1), the average rank was 6, and for about 90% of all residues the sequentially following neighbor had a rank ≤10.

(2) To make sure that the correlation function accounts for the fact that the sequential $d_{\alpha N}$ and d_{NN} NOE cross peaks are the most reliable indicators of sequential proximity (Billeter et al., 1982), the intraresidual ^{15}N-H^N and H^N-H^α peaks of residue s should have high intensity in the predicted pattern for the sequentially neighboring strip, $\vec{v}_{s+1}$. The ^{15}N-H^N peak is usually the strongest peak in a strip, so that no further emphasis is needed, but selective upscaling of the H^N-H^α peak (Fig. 2E) was found to improve the results significantly. Furthermore, to reduce possible errors arising in case of accidental overlap of the intraresidual H^N-H^α peak with the sequential $d_{\alpha N}$ peak, these intraresidual peaks are selectively downscaled in all strips $\vec{v}_k$ (Fig. 2F). These selective intensity scalings are implemented by replacing Eq. 2 by Eq. 3:

$$i_j = \frac{A \cdot i_j^{ex}}{|i_m| + i_b} \qquad (p_l \le j < p_h) \tag{3}$$

with A = 4 for the intraresidual H^N-H^α peak in $\vec{v}_{s+1}$; A = 0.33 for the intraresidual H^N-H^α peak in all $\vec{v}_k$; and A = 1 for all other peaks in $\vec{v}_{s+1}$ and $\vec{v}_k$. In contrast to Eq. 2, which relies entirely on the intensities extracted from the NOESY spectrum, this additional refinement relies on independent knowledge of the intraresidual H^α frequencies. These can be identified, for example, using 3D ^{15}N-correlated [^1H,^1H]-TOCSY. With Eq. 3, the following results were obtained for cyclophilin (Fig. 3C): 63% of the sequential neighbors had rank 1, the average rank for neighboring residues was 3.6, and for 91% of all residues the sequentially following neighbor had a rank ≤5.

The performance of the correlation function can in principle be further improved by eliminating or reducing contributions from experimental artifacts, either by automated or interactive corrections. For example, between residues with similar amide proton chemical shifts the diagonal ^{15}N-H^N peaks contribute to C(s+1,k), although they contain no information on sequential relations. We introduced an automated correction for the case that the separation of the diagonal peaks in v_{s+1} and v_k is smaller than Δp_d. The intensities i_j over the range Δp_d centered over the two diagonal peaks are then set to zero. However, using $\Delta p_d = 3$ data points, only very small further improvements were obtained with the proteins of Fig. 4. Furthermore, for the case that certain strips contain nonrandom noise patterns, the performance of the correlation function may be improved by interactive downscaling of the intensities i_j over such spectral regions in the strips $\vec{v}_k$ concerned. Facilities for such corrections upon visual examination of the strips are implemented in XEASY.

RESULTS AND DISCUSSION

The overall performance of the spectral correlation method introduced in the preceding section is illustrated in Fig. 4, where the results for five different ^{15}N-labeled proteins are shown in the

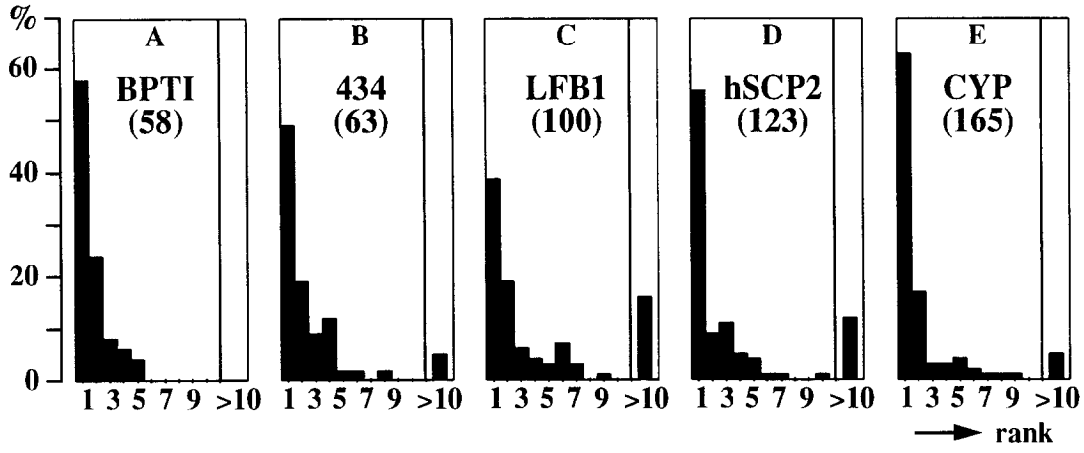

Fig. 4. Results obtained using the spectral correlation function with Eqs. 1 and 3 for sequence-specific assignments of five different proteins. For all these proteins the same parametrization of the correlation function was used, with A as given below Eq. 3 and i_b=1500. The histograms show the percentages of actual sequential neighbors that were attributed ranks 1–10 and >10 with the use of Eq. 1. In all cases, only the ^{15}N-correlated [^{1}H,^{1}H]-NOESY spectra and the chemical shift of the intraresidual H^N-H^α cross peaks determined by ^{15}N-correlated [^{1}H,^{1}H]-TOCSY spectra were used in the analysis. In each histogram the number in parentheses indicates the number of residues in the protein studied: (A) ^{15}N-labeled bovine pancreatic trypsin inhibitor; (B) ^{15}N-labeled fragment 1–63 of the 434 repressor; (C) a ^{15}N-labeled 100-residue polypeptide containing the fragment 195–286 of the LFB1/HNF1 transcription factor from rat liver in positions 5–96 (Leiting et al., 1993); (D) ^{15}N-labeled human sterol carrier protein-2 (Szyperski et al., 1993); (E) ^{15}N-labeled human cyclophilin A, complexed with cyclosporin A (Wüthrich et al., 1991; Spitzfaden et al., 1994).

form of histograms of the ranks of the C-terminal sequential neighbors. For the 58-amino acid protein bovine pancreatic trypsin inhibitor (BPTI), which contains mostly β-sheet secondary structure (Berndt et al., 1992), the method worked almost perfectly, with 58% of the neighboring non-proline residues in rank 1 (Fig. 4A). The size of the protein is not critical, since the distribution obtained for the 165-amino acid protein cyclophilin is similar to that for BPTI, with 63% of neighboring residues ranked 1 (Fig. 4E). The method works for different types of secondary structure, as is shown by the fact that a good result, with 49% of the neighboring residues ranked 1, was obtained also for the 434 repressor (Fig. 4B), which is an α-protein (Neri et al., 1992). Significantly poorer results were obtained for the human sterol carrier protein-2 and for a homeodomain-containing fragment of the LFB1/HNF1 transcription factor from rat liver (Fig. 4C and D). These two proteins have extensive unstructured chain-terminal segments (Leiting et al., 1993; Szyperski et al., 1993). The residues for which the spectral correlation method worked less well are predominantly located in these disordered regions of the polypeptide chain, indicating that conformational flexibility is the main reason for the observed reduced performance of Eqs. 1 and 3 with these two proteins. For the well-structured region of residues 16–85 in LFB1, 78% of the neighboring residues were ranked 1 and 8% had rankings >10, and for the well-structured residues 4–104 in hSCP the corresponding numbers are 65% and 4%.

Using the spectral correlation approach in practice, one will have access to additional information besides 3D ^{15}N-correlated [^{1}H,^{1}H]-NOESY, similar to the situation encountered with interactive assignments. In particular, corresponding 3D heteronuclear-resolved COSY and/or TOCSY spectra will be compared with NOESY to identify intraresidual cross peaks, which is readily

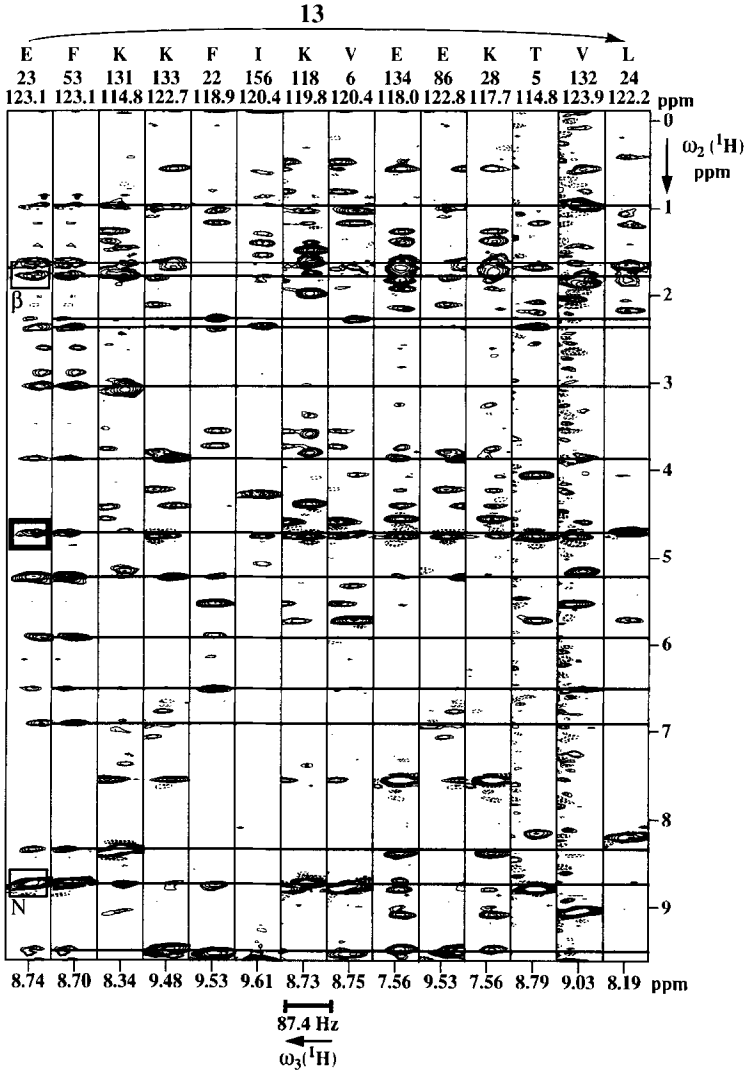

Fig. 5. A similar strip plot as in Fig. 1, taken from the 3D ^{15}N-correlated [^{1}H,^{1}H]-NOESY spectrum of ^{15}N-labeled cyclophilin complexed with cyclosporin A. The strips attributed ranks 1–13 as potential C-terminal sequential neighbors of Glu^{23} are shown (see also Fig. 1).

achieved with the interactive routines of the program XEASY. As an example, 3D ^{15}N-correlated [^{1}H,^{1}H]-TOCSY would be compared with 3D ^{15}N-correlated [^{1}H,^{1}H]-NOESY. For a relevant evaluation of the results, one therefore has to compare the extent and reliability of assignments obtained using the correlation function of Eq. 1 with those that could be obtained interactively from the same experimental data by an experienced spectroscopist. Straightforward use of the sequential NOE technique with globular proteins can yield unambiguous identification of the neighboring residue in about 90% of the cases (Billeter et al., 1982; Wüthrich, 1986). In an interactive approach the remaining ambiguities are usually removed by indirect information, such as identification of individual spin systems combined with consideration of the small selection of

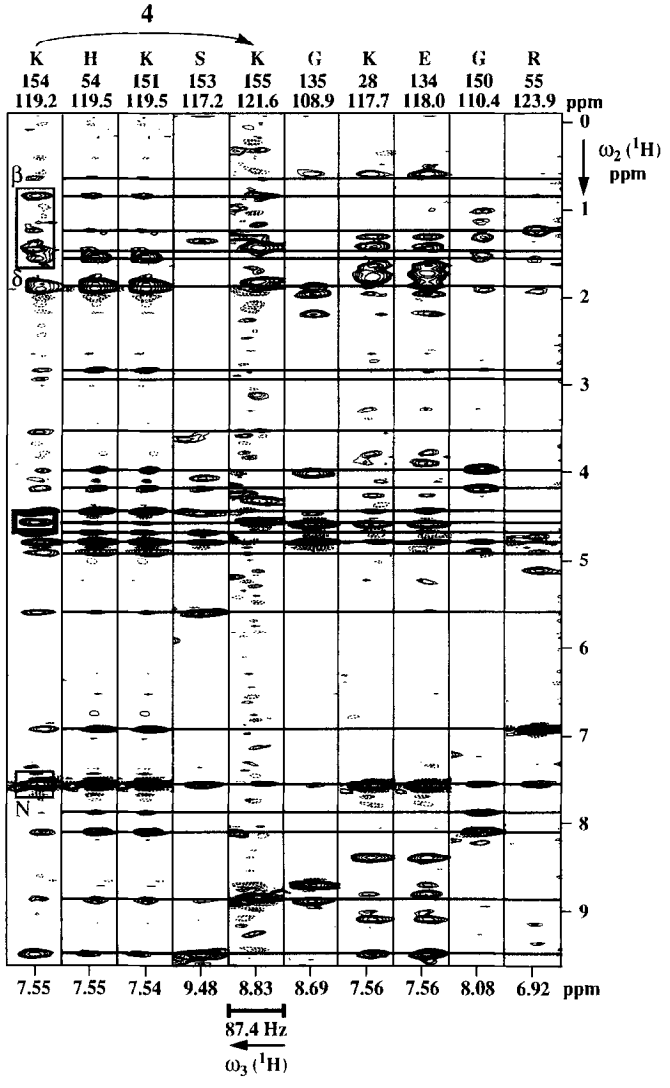

Fig. 6. A similar strip plot as in Fig. 1, taken from the 3D ^{15}N-correlated [^{1}H,^{1}H]-NOESY spectrum of ^{15}N-labeled cyclophilin complexed with cyclosporin A. The strips attributed ranks 1–9 as potential C-terminal sequential neighbors of Lys^{154} are shown (see also Fig. 1).

unassigned residues left toward the end of the assignment process. An optimal correlation function could thus find first ranks for about 90% of all neighboring residues. It is, however, more important that the highest possible percentage of all sequential neighbors is highly ranked, say, 1 to 5 or even 1 to 10, since the rankings obtained with Eq. 1 are in practice used as the starting point for a drastically abbreviated interactive assignment procedure. In the following we investigate the relative potentialities of the correlation function and the conventional interactive approach for two specific residue pairs in cyclophilin.

Figure 1 contains a poor ranking for the dipeptide segment Glu^{23}-Leu^{24}. This situation is

further analyzed in Fig. 5 by a display of all the strips for which Eq. 1 attributed the ranks 1 to 13 relative to Glu^{23}. It is readily apparent that the failure to attribute a low rank to Leu^{24} is due to the absence of well-resolved sequential NOEs. In the strip of Leu^{24} the sequential $d_{\alpha N}$ peak overlaps with the strong intraresidual $d_{N\alpha}(i,i)$ peak, and there is not a single peak that has its maximum intensity at the positions of the horizontal lines drawn through the peak centers in the strip of Glu^{23}. Such lack of sequential NOE connectivities may generally arise from low signal-to-noise ratio, possibly caused by slow conformational fluctuations in the protein and concomitant line broadening, accidental overlap of peaks, or the presence of artifacts or strong noise bands. In such cases the spectral correlation method will attribute lower ranks to any strip $\vec{v}_k$ containing at least one strong peak that overlaps with a peak in strip $\vec{v}_s$ than to the actual sequential neighbor (see Fig. 5). As mentioned above, in such a case the sequential connectivity cannot be established without using additional information, independent of whether an interactive approach or the correlation function is used.

In Fig. 6 a neighboring strip was not attributed rank 1, although both sequential NOEs $d_{\alpha N}$ and d_{NN} are represented by well-separated peaks. It should be emphasized that such cases are normally recognized as rank 1 by Eq. 1, and in all the proteins studied so far it never occurred that a strip containing at least one well-resolved sequential peak $d_{\alpha N}$ or d_{NN} was not identified in the first 10 ranks. In the case shown here, the imperfect rankings by the correlation function were due to the nearly identical H^N and ^{15}N chemical shifts of Lys^{154}, His^{54} and Lys^{151}, and the fact that the sequentially preceding residue Ser^{153} has a strong d_{NN} peak (Fig. 6). In the proteins studied so far, sequentially preceding residues with outstandingly strong d_{NN} peaks repeatedly were attributed a lower rank than the sequentially following residue, which is due to the fact that d_{NN} connectivities are expected for both sequentially neighboring residues (Billeter et al., 1982). This situation can usually be rectified by reference to the amino acid sequence and additional information from the $d_{\alpha N}$ and $d_{\beta N}$ peaks. We also noted that residues from adjacent β-strands are sometimes attributed low ranks. For example, Lys^{131} and Lys^{133} in cyclophilin are located in the β-strand next to the one containing Glu^{23} (Fig. 5). Overall, all these adverse situations pose the same problems for assignments either by an unguided interactive approach or by the correlation function, and will in both procedures be clarified with the use of additional information on spin systems and the amino acid sequence (Wüthrich, 1986).

CONCLUSIONS

The presently proposed correlation function yields correct identifications of sequentially neighboring residues to a comparable extent as the conventional interactive approach, and with its implementation in the software package XEASY it enables efficient resonance assignments in ^{15}N-labeled proteins using 3D ^{15}N-correlated [^1H,^1H]-NOESY combined with corresponding 3D heteronuclear-resolved COSY- and/or TOCSY-type experiments for identification of intraresidual connectivities. The method should be applicable to larger, well-structured proteins, considering that heteronuclear-correlated [^1H,^1H]-NOESY spectra have good sensitivity and that the approach is robust with regard to spectral degeneracies, since sequential connectivities are usually established by multiple NOE peaks (see Figs. 1, 5 and 6).

Similar correlation function approaches can be implemented for computer-supported analysis of other types of NMR spectra. For example, in HCCH-TOCSY experiments the group of strips

originating from the different protons of a given spin system should be readily identified using a correlation function with suitably weighted peak intensities in the individual strips.

ACKNOWLEDGEMENTS

Financial support was obtained from the Kommission zur Förderung der wissenschaftlichen Forschung (project 2223.1) and the Schweizerischer Nationalfonds (project 31.32033.91). We thank S. Altmann, Dr. G. Siegal, O. Schott, Dr. C. Spitzfaden and Dr. T. Szyperski for the use of so far unpublished spectra of the ^{15}N-labeled proteins in Fig. 4, Dr. M. Billeter for helpful discussions, and Mrs. E. Huber for the careful processing of the manuscript.

REFERENCES

Bax, A. and Grzesiek, S. (1993) *Acc. Chem. Res.*, **26**, 131–138.
Berndt, K.D., Güntert, P., Orbons, L.P.M. and Wüthrich, K. (1992) *J. Mol. Biol.*, **227**, 757–775.
Billeter, M., Braun, W. and Wüthrich, K. (1982) *J. Mol. Biol.*, **155**, 321–346.
Driscoll, P.C., Clore, G.M., Marion, D., Wingfield, P.T. and Gronenborn, A.M. (1990) *Biochemistry*, **29**, 3542–3556.
Eccles, C., Güntert, P., Billeter, M. and Wüthrich, K. (1991) *J. Biomol. NMR*, **1**, 111–130.
Gao, X. and Burkhart, W. (1991) *Biochemistry*, **30**, 7730–7739.
Leiting, B., De Francesco, R., Tomei, L., Cortese, R., Otting, G. and Wüthrich, K. (1993) *EMBO J.*, **12**, 1797–1803.
Neri, D., Billeter, M. and Wüthrich, K. (1992) *J. Mol. Biol.*, **223**, 743–767.
Rico, M., Bruix, M., Santoro, J., González, C., Neira, J.L., Nieto, J.L. and Herranz, J. (1989) *Eur. J. Biochem.*, **183**, 623–638.
Spitzfaden, C., Braun, W., Wider, G., Widmer, H. and Wüthrich, K. (1994) *J. Biomol. NMR*, **4**, 463–482.
Szyperski, T., Scheek, S., Johansson, J., Assmann, G., Seedorf, U. and Wüthrich, K. (1993) *FEBS Lett.*, **335**, 18–26.
Wagner, G. and Wüthrich, K. (1982) *J. Mol. Biol.*, **155**, 347–366.
Wüthrich, K. (1986) *NMR of Proteins and Nucleic Acids*, Wiley, New York, NY.
Wüthrich, K. (1989) *Science*, **243**, 45–50.
Wüthrich, K., Wider, G., Wagner, G. and Braun, W. (1982) *J. Mol. Biol.*, **155**, 311–319.
Wüthrich, K., Spitzfaden, C., Memmert, K., Widmer, H. and Wider, G. (1991) *FEBS Lett.*, **285**, 237–247.